Expert Systems with Applications 36 (2009) 8631–8638

Contents lists available at ScienceDirect

Expert Systems with Applications

journal homepage: www.elsevier.com/locate/eswa

Predicting of fan speed for energy saving in HVAC system based on adaptive network based fuzzy inference system

Servet Soyguder *, Hasan Alli

Firat University, Department of Mechanical Engineering, 23279 Elaziğ, Turkey

ARTICLE INFO

Keywords:
HVAC system
Fan motor speed predicting
Air flow control
Energy saving
Temperature control
PID control
ANFIS

ABSTRACT

In this paper, a HVAC (heating, ventilating and air-conditioning) system has two different zones was designed and fan motor speed to minimize energy consumption of the HVAC system was controlled by a conventional (proportional–integral-derivative) PID controller. The desired temperatures were realized by variable flow-rate by considering the ambient temperature for each zone. The control algorithm was transformed for a programmable logic controller (PLC). The realized system has been controlled by PLC used PID control algorithm. The input–output data set of the HVAC system were first stored and than these data sets were used to predict the fan motor speed based on adaptive network based fuzzy inference system (ANFIS). In simulations, root-mean-square (RMS) and the coefficient of multiple determinations (R^2) as two performance measures were obtained to compare the predicted and actual values for model validation. All simulations have shown that the proposed method is more effective and controls the systems quite well.

1. Introduction

The comfort of the people in their living environment is partially dependent on the quality and temperature of air in their building. Three interrelated systems are used to provide the desired air temperature and quality. These are the ventilating system, the heating system and the air conditioning system. The purpose of HVAC system of a building is to provide complete thermal comfort for its occupants. On the other hand, energy saving in this system is one of the most important issue because of its cost. Hence, it is necessary to understand the aspects of minimum energy consumption in order to design an effective HVAC system.

Teitel, Levi, Zhao, Barak, Bar-lev and Shmuel have employed for variable frequency drives method which is routinely used to vary pump and fan motor speed in heating, ventilating and air conditioning of buildings (Teitel et al., 2008). In these applications, speed control is used to regulate the flow of water or air because speed adjustment is an energy efficient method of flow control. The aim of this study is to present a thermodynamic model for an air-cooled centrifugal chiller which is developed specifically to analyze how the speed control of the condenser fans influences the chiller's COP under various operating conditions (Yu & Chan, 2006, 2007). Moreover, the other study of the same authors is made to investigate how the use of variable speed condenser fans enables air-cooled chillers to operate more efficiently (Yu & Chan, 2006, 2007). Besides, variable fan speed control is increasingly used for chiller compressors to save power when chillers are operating at part load. The power saving comes from the improved efficiency of the motors when operating at a lower speed under part-load conditions (Aprea, Mastrullo, Renno, & Vanoli, 2004; Tassou & Quereshi, 1998).

HVAC systems require control of environmental variables such as pressure, temperature, humidity. Furthermore, HVAC system is necessary to implement a realistic thermal environment in terms of temperature and air flow rate in the space of virtual reality (Shin, Chang, & Kim, 2002; Kaynakli, Pulat, and Kilic, 2005). As in other industrial applications, most of the controllers commissioned in HVAC systems are of the proportional–integral-derivative (PID) type (Bi et al., 2000; Seem, 1998). This is mainly because PID is simple yet sufficient for most HVAC application specifications. However, tuning a PID controller requires an accurate model of a process and an effective controller design rule. In addition to that, the tuning procedure can be a time-consuming, expensive and difficult task (Bi et al., 2000; Krakow & Lin, 1995; Pinnella, Wechselberger, Hittle, & Pederson, 1986; Riverol & Pilipovik, 2005).

The developments in intelligent methods make them possible to use in nonlinear analysis and control. Intelligent methods were first used to increase the robustness of existing models however they have been used to obtain new models in recent years. In addition to PID control of HVAC systems, the various studies using intelligent methods were presented. A neural network (NN) model was developed to predict air pressure coefficients across the openings in a light weight, single sided, naturally ventilated test room

* Corresponding author. Tel.: +90 424 2370000x5330; fax: +90 424 2415526.
E-mail addresses: ssoyguder@firat.edu.tr (S. Soyguder), halli@firat.edu.tr (H. Alli).

0957-4174/$ - see front matter © 2008 Elsevier Ltd. All rights reserved.
doi:10.1016/j.eswa.2008.10.033

Nomenclature

A	area (m^2)
$\dot{m}_{ca}$	the mass flow-rate in fan channel (kg/h)
$\dot{m}_{z1a,in}$	the mass flow-rate entered to Zone-1 (kg/h)
$\dot{m}_{z2a,in}$	the mass flow-rate entered to Zone-2 (kg/h)
$\dot{m}_{sva,out}$	the mass flow-rate exist from safety valve (kg/h)
$\dot{m}_{exha,out}$	the mass flow-rate exist from exhaust (kg/h)
Q	convection and transmission heat (J)
W	Work (J)
$\dot{m}_{z1a,in} = \dot{m}_{Za}$	the mass flow-rate entered to Zone-1 (kg/h)
h_{in}	specific enthalpy(J/kg)
h_{out}	specific enthalpy (J/kg)
U	the internal energy (J)
C_v	constant heat (kJ/kg K)
C_p	constant pressure (kJ/kg K)
T	inner temperature (°C)
T_n	instant temperature (°C)
T_{n-1}	vicious circle temperature (°C)
$T_{sh,gir}$	cool air temperature (°C)
T_{out}	outside temperature (°C)
T_{eva}	evaporator temperature (°C)
h_{out}	convection coefficient for outside-surface (J/m^2 K)
h_{in}	convection coefficient for inner-surface (J/m^2 K)
K	transmission coefficient (J/m K)
L_1	thickness for Zone-1 (m)
L_2	thickness for Zone-2 (m)
M_n	calculated value of the loop output at sample time n
K_p	the loop gain
K_i	proportional constant of the integral term
K_d	proportional constant of the differential term
c_f	flow discharge coefficient
$\Delta\rho$	relatively constant
M_{in}	initial value of the loop output
e_n	value of the loop error at sample time n
e_{n-1}	previous value of the loop error
e_x	value of the loop error at sample time x
O_i	output of ANFIS layer
A_i	linguistic label
w_i	firing strength of rules
RMS	root-mean square error
R^2	fraction of variance
$y_{pre,m}$	predicted value
$t_{mea,m}$	measured value

(Kalogirou, Eftekhari, & Marjanovic, 2003). The applicability of natural ventilation as a passive cooling system was investigated in modern buildings in Kayseri using model simulations of indoor air velocity by the fluent. Using the simulated data, an ANFIS model was employed to predict the indoor average and maximum air velocities (Ayata, Çam, & Yıldız, 2007). A systematic approach for optimal set point control for in-building section was presented (Lu, Wenjian, Lihua, Shujiang, & Chai, 2005). The major components of in-building section were analyzed to identify the energy conservation potential. In order to save energy for delivery of supply air and chilled water, a variable pressure set point method was analyzed by a simple example and an intelligent neural network model-ANFIS was proposed to compute the variable pressure set points influenced by variation of cooling loads of end users. In addition, fuzzy logic control (FLC) of HVAC systems was studied by many authors (Huang & Nelson, 1994). The obtained results were compared with those of PID control and these studies indicated that FLC had better results. FLC is extensively used in processes where systems dynamics is either very complex or exhibit highly nonlinear characters. Besides, FLC is one of useful control schemes for plants having difficulties in deriving mathematical models or having performance limitations with conventional linear control methods. FLC is designed on the basis of human experience that means a mathematical model is not required for controlling a system. Because of this advantage, fuzzy logic-based control schemes were implemented for many industrial applications (Hung, Lin & Chung; 2007; Tang & Mulholland, 1987). FLCs were successfully applied to many complex industrial processes and domestic appliances in recent years (Tsang, 2001). The first FLC algorithm implemented by Mamdani was designed to synthesize the linguistic control protocol of an experienced operator (Mamdani, 1974). Consequently, different control tuning methodologies have been proposed in the literature such as auto-tuning, self-tuning, artificial intelligence, and optimization methods.

In this study, based on considering the above literatures, the required fan motor speed to minimize energy consumption and the required damper gap rates for obtaining the desired temperatures of two different zones for each time step were found by using PID control algorithm. The damper gap rate is also proportional with air flow rate. Besides, in this study, an expert system for fan motor speed and air flow control of HVAC system based on ANFIS is presented. In simulations, root-mean-square (RMS) and the coefficient of multiple determinations (R^2) as two performance measures are given to compare the predicted and actual values for model validation. All simulations have shown that the proposed method is more effective and controls the systems quite well.

The outline of the paper is as follows. In Section 2, the model of the HVAC system is presented. The design of the considered real-time HVAC system is given Section 3. Section 4 briefly describes the adaptive network based fuzzy inference system (ANFIS). Then, in Section 5, the experimental results are presented. In the experiment, the fan motor speed and the damper gap rate being proportional with air flow rate has been controlled using PID controllers and ANFIS. Finally, conclusions are given in Section 6.

2. The model of the HVAC system

Fig. 1 shows the schematic diagram of the modeled system in this study. The main elements of the system: The cooling zone-areas, evaporator, cooling unit, fan, damper motors, channels, thermocouples. Obtaining of the mathematical model of the cooled zone by considering all parameters is quite difficult. Fort this reason, we consider the following assumptions:

(1) The effect of the instantaneous variations of air speed in the zones on the pressure is neglected.
(2) There is no air leakage except the exhaust valves of the zones.
(3) The air flow in the zones is homogeneous.

The mass flow-rate ($\dot{m}_{ca}$) absorbed from the cooling unit does not change because the supply fun has constant the number of revolution. However, the mass flow-rate of the air entering to the zones changes depending on the temperatures of the zones. The continuously variations of the input mass flow-rate ($\dot{m}_{z1a,in}$) Zone-1 and ($\dot{m}_{z2a,in}$) Zone-2 are realized by regulating the gap rates of dampers into the entrances of zone-channels, depending on the control output signals.

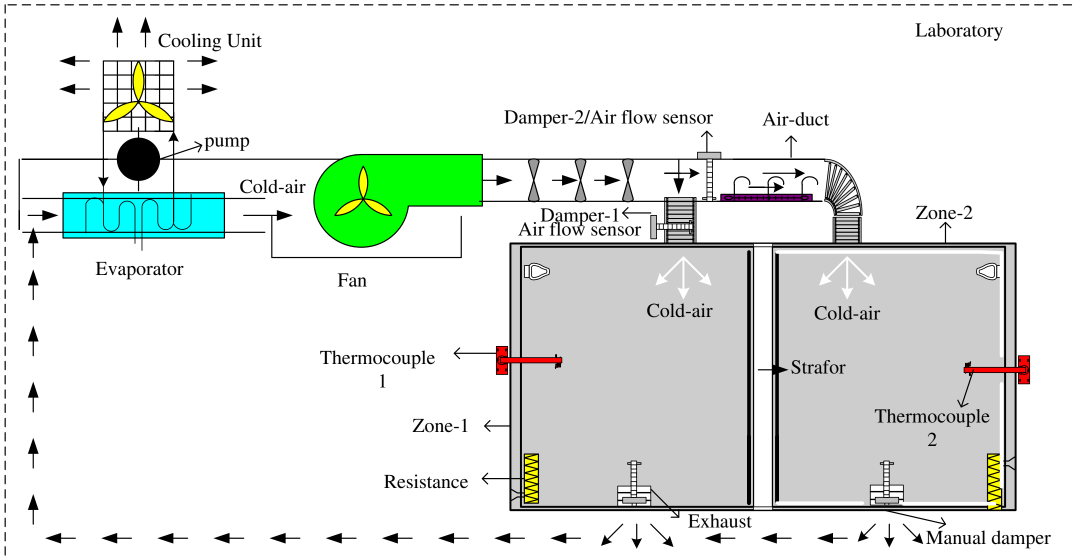

Fig. 1. The schematic view of the HVAC system having two zones.

The continuity equation of the controlled system can be formed as:

$$\dot{m}_{ca} = \dot{m}_{z1a,in} + \dot{m}_{z2a,in} + \dot{m}_{sva,out}. \tag{1}$$

The mass flow-rate $\dot{m}_{sva,out}$ in Eq. (1) belongs to the safety valve discharging the excessive air coming from the zones.

There is no change in the flow-rates of the zones since the input flow-rate equals to the output flow-rate. That's why we can write the continuity equation as:

$$\dot{m}_{za,in} = \dot{m}_{exha,out} = \dot{m}_{za}. \tag{2}$$

According to thermodynamic first law, the internal energy equation can be stated as follows:

$$Q - W + \sum \dot{m} + za,in \cdot h_{in} - \sum \dot{m}_{exha,out} \cdot h_{out} = \frac{du}{dt}, \tag{3}$$

where u represents time-dependent variation of heat. Furthermore, Eq. (3) can be re-written as the following form, assuming that there is no work in the system.

$$Q + \dot{m}_{za} \cdot (h_{in} - h_{out}) = \frac{du}{dt} = \frac{m_{za} \cdot C_v \cdot (T_{n-1} - T_n)}{dt}, \tag{4}$$

$$h_{in} - h_{out} = C_p \cdot (T_{ca,in} - T_n). \tag{5}$$

If Eq. (4) is rearranged, we get:

$$Q + \dot{m}_{za} \cdot C_p.(T_{ca,in} - T_n) = \frac{m_{za} \cdot C_v \cdot (T_{n-1} - T_n)}{dt}, \tag{6}$$

$$Q + \dot{m} + za \cdot C_p.(T_{ca,in} - T_n) = m_{za} \cdot C_v \cdot \frac{dT}{dt}, \tag{7}$$

where T represents the instantaneous temperature variation. The heat transfer from the outside to the system can be stated as:

$$Q = \frac{T_{out} - T_n}{R} \tag{8}$$

or

$$Q = \frac{T_{out} - T_n}{\frac{1}{h_{out} \cdot A} + \frac{L_1}{k_1 \cdot A} + \frac{L_2}{k_2 \cdot A} + \frac{1}{h_{in} \cdot A}} \tag{9}$$

If Eq. (9) is substituted in Eq. (8), we get:

$$\frac{dT}{dt} = \frac{Q + \dot{m}_{za} \cdot C_p(T_{ca,in} - T_n)}{m_{za} \cdot C_v}. \tag{10}$$

3. The design of the considered real-time HVAC system

In this experimental study, the cooling process was performed for the two zones having the different properties as shown in Fig. 2a and b. The volume of the each zone has 0.5 m^3. The all surface areas of Zone-1 were isolated with the isolation materials (strafor) while those of Zone-2 were not. The aim of this choice is to clearly see the steady-state differences to obtain the reference temperatures. The cooled air transfer has been realized from the main channel having the supply fan to the region of Zone-1 and Zone-2 as seen in Fig. 2a and b. The channel flow cross-section area is 0.02 m^2. The 0° position of the damper (opening angle (θ)) is the full open position and the system has the maximum air mass flow-rate. Maximum air mass flow rate is 50 kg/h for the 0° position of the damper (opening angle (θ)). Air mass flow rate is direct proportional with opening angles (θ) between the 0° position of the damper and the 90° position of the damper. At the same time, air mass flow rate is direct proportional with fan motor speed Furthermore, fan motor speed is dependent on evaporator temperature, as seen from the block diagram in Fig. 3. The 90° position of the damper is the closed position of the damper and the cooled air can not pass through the zones. Air mass flow rate is controlled by a stepper-driven throttle damper-valve. The relationship between the damper-valve opening θ and the air mass flow rate through the damper-valve $\dot{m}_{za}$ is expressed as

$$\dot{m}_{za} = c_f \sqrt{\rho \Delta p} A(\theta), \tag{11}$$

where c_f and A are flow discharge coefficient and flow cross-section area, respectively. In the expression, the pressure drop across the damper $\Delta\rho$ is relatively constant because the static pressure in the loop is self-regulated due to the characteristics of the fan that would maintain the static pressure at which fan power balances with the circulation flow rate in the loop (McQuiston & Parker, 1997). In that case, the mass flow rate $\dot{m}_{za}$ is mainly proportional to the flow area $A(\theta)$ according to the experimental data shown in Figs. 11–13.

The evaporator and the air compressor were used for cooling the system and the required air flow was supplied by controlled

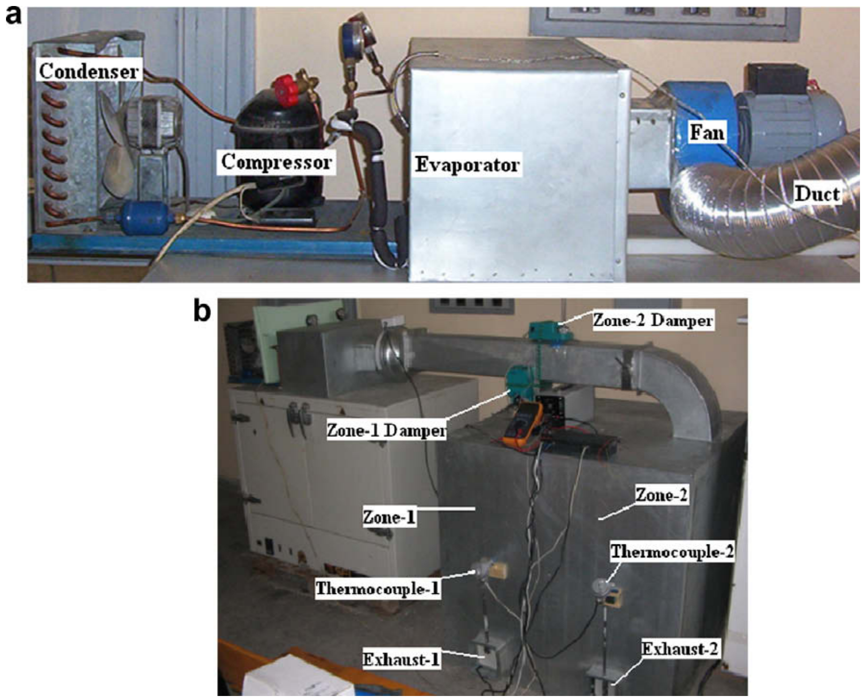

Fig. 2. (a) and (b) A prototype of the real-time HVAC system experimental setup.

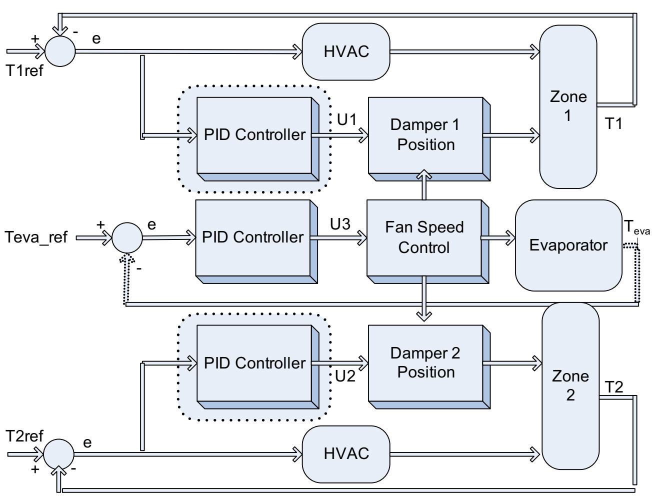

Fig. 3. The block diagram of the considered system.

of the dampers placed on the entrance ducts of each zone. There are the damper motors in the entrances of the each zone, controlled by PID control algorithm, as seen from the block diagram in Fig. 3. The air supply fan first absorbs 5 °C air from the evaporator, then sends to the zones. In this study, the fan motor speed is also controlled by PID control algorithm to minimize energy consumption, as seen from the block diagram in Fig. 3.

4. Adaptive network based fuzzy inference system (ANFIS)

The architecture and learning rule of ANFIS have been described in detail. ANFIS is a Multilayer feed forward network where each node performs a particular function on incoming signals. Both square and circle node symbols are used to represent different properties of adaptive learning. To perform desired input–output characteristics, adaptive learning parameters are updated based on gradient learning rules. ANFIS model is one of the implementation of a first order Sugeno fuzzy inference system (Jang, 1993; Kulakarni, 2001). The rules are of the form Eq. (12). In this system,

$$\text{If } (x1 \text{ is } A1, x2 \text{ is } A2, \text{ then } y = px1 + qx2 + r), \tag{12}$$

where $x1$ and $x2$ are inputs corresponding $A1$ and $A2$ term set, y is output, p, q, r are constant. An ANFIS model is shown in Fig. 4. It is a multi-input, one-output model however a multi-output model can be designed by connecting few single output models. The node functions in the same layer are similar and described as below.

Layer-1: Every node i in this layer is a square node with a node function. Nodes in layer 1 implement fuzzy membership functions, mapping input variables to corresponding fuzzy membership values. Outputs of this layer can be described

$$O_i^1 = \mu A_i(x), \tag{13}$$

where x is input to node i, and A_i is linguistic label associated with this node function. O_i^1 is the membership function of A_i and the fuzzy membership functions (MF) can take any form, such as triangular, Gaussian but usually $\mu A_i(x)$ is chosen bell-shaped with maximum equal 1 minimum equal 0.

Layer-2: Every node in this layer is a circle node labeled Π which multiplies the incoming signals and sends the product out. For instance,

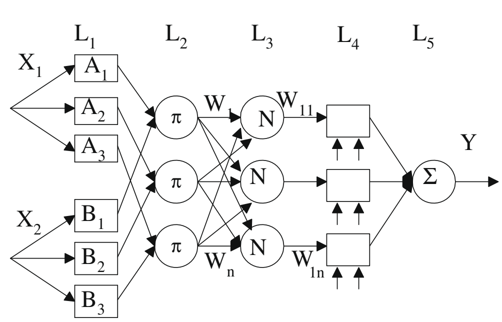

Fig. 4. ANFIS model structure.

$$W_i = \mu A1(x)^* \mu A2(y) \ldots \quad i = 1, 2, 3, \ldots N. \tag{14}$$

Each node output represents the firing strength of a rule.

Layer-3: Every node in this layer is a circle node labeled N. The ith node calculates the ratio of the ith rules firing strength to the sum of all rule's firing strengths. Where $\bar{w}$ is the normalized firing strength of rules.

$$\bar{w}_i = \frac{w_i}{w_1 + w_2 + \cdots + w_N} \quad i = 1, 2, 3, \ldots, N. \tag{15}$$

Layer-4: Every node i in this layer is a square node with a node function,

$$O_i^4 = \bar{w}_i f_i = \bar{w}_i(px + qy + \cdots + r) \quad i = 1, 2, 3, \ldots, N, \tag{16}$$

where $\bar{w}_i$ is the output of layer 3 and $\{p, q, r\}$ is the parameter set. Parameters in this layer are referred to as consequent parameters.

Layer-5: The single node in this layer is a circle node labeled $\sum$ that computes the overall output of ANFIS as the summation of all incoming signals.

$$O_i^5 = \text{overall output} = \sum_i \bar{w}_i f_i = \frac{\sum_i w_i f_i}{\sum_i w_i}. \tag{17}$$

5. Experimental results

In the experiment, air mass flow rate has been controlled by fan motor speed and dampers using PID controllers. The experimental results were taken for the same PID parameters (Kp = 14.53 proportional – Ki = 0.13 integral – Kd = 0.01 derivative for Zone-1, Kp = 15.28 proportional – Ki = 0.17 integral – Kd = 0.01 derivative for Zone-2 and Kp = 13.81 proportional – Ki = 0.12 integral – Kd = 0.01 derivative for evaporator obtained by Ziegler and Nichols (Z–N) methods. The ambience temperature was approximately 26.4 °C for each application. The set temperature values of Zone-1 and Zone-2 have been adjusted as 22.0 °C and 23.0 °C, respectively. Besides, the required set temperature values of evaporator have been adjusted as 5 °C. The set temperature of evaporator (5 °C) is theoretically taken in thermodynamic applications. The most important duration in HVAC systems is steady-state time which approximately contains three quarters of all day. The obtained results are presented in graphical form as seen in Figs. 5–7.

The realized HVAC systems data were used in this study to train and test the ANFIS models. All program codes were written by using MATLAB Programme. Three ANFIS models were performed. The proposed modeling structure is shown in Fig. 8. The first one of them is for Zone-1, the second one is for Zone-2 and the third one is for the evaporator. Half of the each zone data were used to training stages and the other parts were used to test stages. The set temperature of zone, the difference between the set temperature of zone and the ambient temperature and the first derivation of the difference between the set temperature of zone and the ambient temperature were used as input to the ANFIS model of zones and damper gap rate was used as ANFIS model output. Besides, the set temperature of evaporator, the difference between the set temperature of evaporator and the evaporator temperature and the first derivation of the difference between the set temperature of evaporator and the evaporator temperature were used as input to the ANFIS model of evaporator and fan motor speed was used as ANFIS model output. So each ANFIS model has three inputs and one output. Different membership functions (MFs) were used and their performances were tabulated and compared. These MFs were tabulated in Table 1.

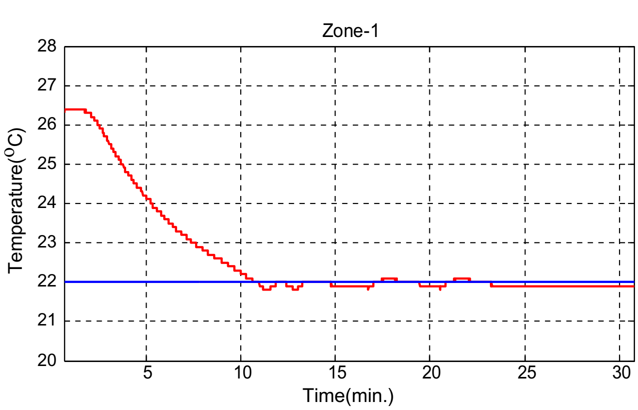

Fig. 5. The set temperature values of Zone-1 [°C].

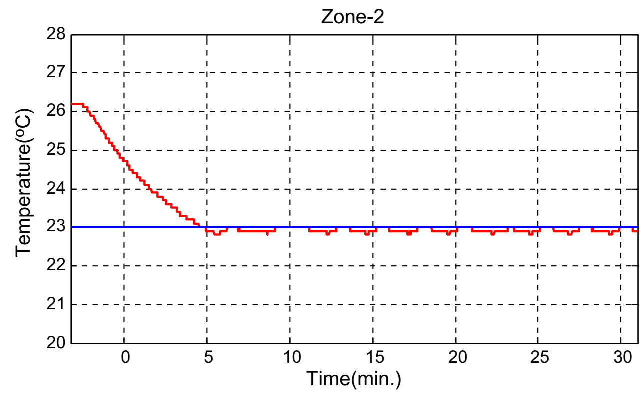

Fig. 6. The set temperature values of Zone-2 [°C].

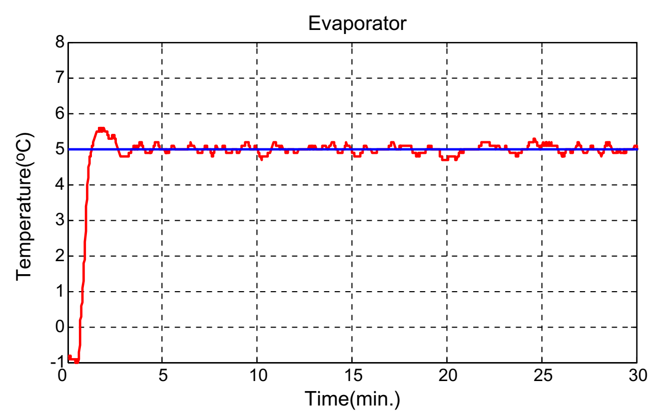

Fig. 7. The set temperature values of evaporator [°C].

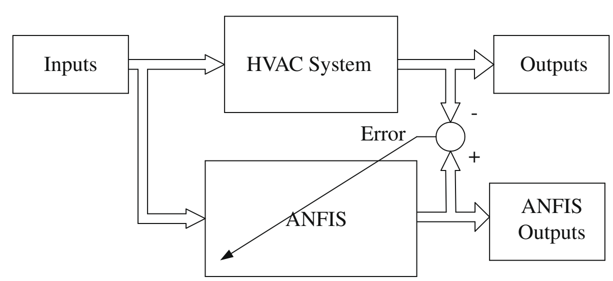

Fig. 8. The block diagram of the proposed intelligent models.

Some statistical methods, such as the root-mean squared (RMS), the coefficient of multiple determinations R^2 are used to compare the predicted and actual values for model validation. The RMS and R^2 can be evaluated by Eqs. (18) and (19), respectively.

Table 1
Membership functions.

Type of MF	Descriptions
PIMF	Pi-shaped curve membership function
TRIMF	Triangular membership function
GBELLMF	Generalized bell curve membership function
GAUSSMF	Gaussian curve membership function
GAUSS2MF	Two-sided Gaussian membership function

$$\mathrm{RMS} = \sqrt{\frac{\sum_{m=1}^{n} (y_{\mathrm{pre,m}} - t_{\mathrm{mea,m}})_2}{n}}, \tag{18}$$

$$R^2 = 1 - \frac{\sum_{m=1}^{n} (y_{\mathrm{pre,m}} - t_{\mathrm{mea,m}})^2}{\sum_{m=1}^{n} (t_{\mathrm{mea,m}})^2}, \tag{19}$$

where n is the number of data patterns in the independent data set, $y_{\mathrm{pre,m}}$ indicates the predicted, $t_{\mathrm{mea,m}}$ is the measured value of one data point m, and is the mean value of all measured data points.

For modeling evaporator; the formed ANFIS model was trained for 300 epochs and the structure of ANFIS model is presented in Table 2. The predicting performance is shown in Fig. 9. The realized simulations and their predicting performance by using different

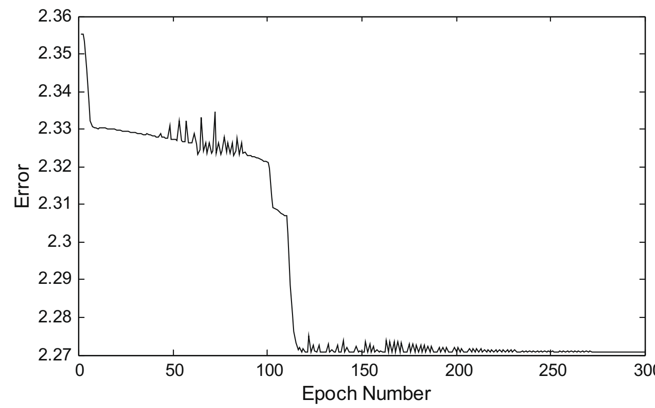

Fig. 10. Training performance of ANFIS model for evaporator.

Table 2
ANFIS model structure for evaporator (Trimf-3).

ANFIS parameters	Values
Number of nodes	78
Number of linear parameters	108
Number of nonlinear parameters	27
Total number of parameters	135
Number of training data pairs	197
Number of fuzzy rules	27

Table 4
ANFIS model structure for zone-1 (Gauss2mf-2).

ANFIS parameters	Values
Number of nodes	34
Number of linear parameters	32
Number of nonlinear parameters	36
Total number of parameters	144
Number of training data pairs	355
Number of fuzzy rules	8

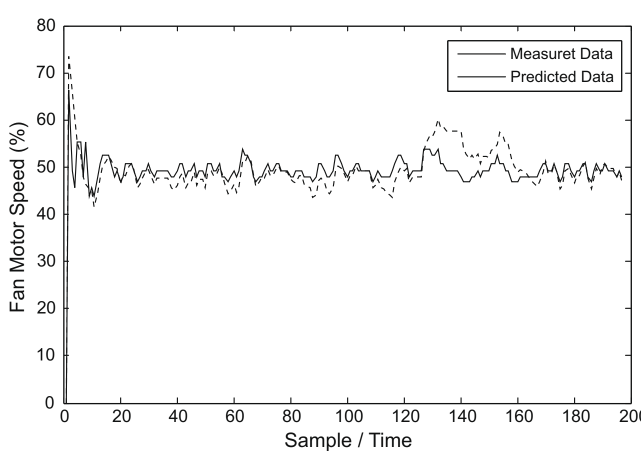

Fig. 9. Predicted and actual fan motor speed (%) for evaporator.

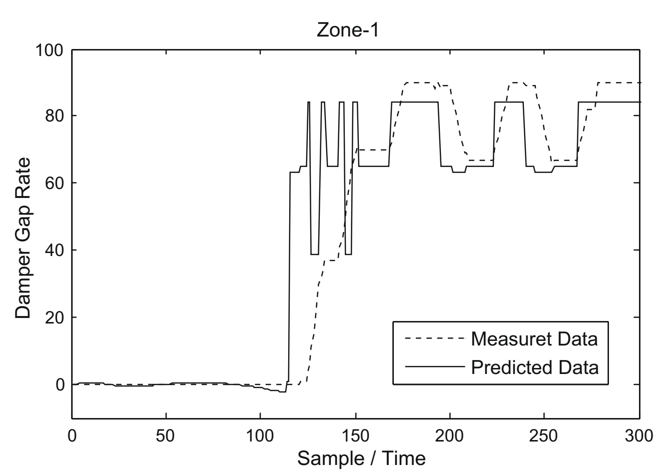

Fig. 11. Predicted and actual gap rate for Zone-1.

Table 3
Predicting performances of ANFIS model with different MFs for evaporator.

Membership Functions	RMS	R^2
Gbellmf-3	7.1817	0.9789
Gbellmf-2	3.3996	0.9953
Trimf-3	**3.3475**	**0.9954**
Trimf-2	3.4674	0.9951
Gaussmf-3	4.8484	0.9904
Gaussmf-2	3.4752	0.9951
Gauss2mf-3	20.4908	0.8282
Gauss2mf-2	20.4928	0.8281
Pimf-3	3.8807	0.9938
Pimf-2	3.9585	0.9936

Table 5
Predicting performances of ANFIS model with different MFs for Zone-1.

Membership Functions	RMS	R^2
Gbellmf-3	16.2935	0.9354
Gbellmf-2	16.3506	0.9350
Trimf-3	16.4103	0.9345
Trimf-2	17.0072	0.9297
Gaussmf-3	15.6828	0.9402
Gaussmf-2	16.4156	0.9345
Gauss2mf-3	16.7610	0.9317
Gauss2mf-2	**15.6750**	**0.9402**
Pimf-3	16.7677	0.9316
Pimf-2	18.9403	0.9128

MF are tabulated in Table 3. Finally, the best performance was obtained with pi shaped MF. The RMS value is 3.3475 and the R^2 value is 0.9954. The training error is shown in Fig. 10.

For modeling Zone-1; the formed ANFIS model was trained for 300 epochs and the structure of ANFIS model is presented in Table 4. The predicting performance is shown in Fig. 11. The realized simulations and their predicting performance by using different MF are tabulated in Table 5. Consequently, the best performance was obtained with pi shaped MF. The RMS value is 15.6750 and the R^2 value is 0.9402. The training error is shown in Fig. 12.

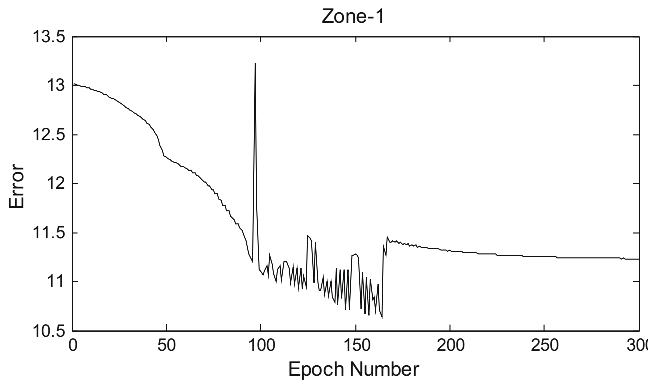

Fig. 12. Training performance of ANFIS model for Zone-1.

Table 6
ANFIS model structure for Zone-2 (Gauss2mf-3)

ANFIS parameters	Values
Number of nodes	78
Number of linear parameters	108
Number of nonlinear parameters	36
Total number of parameters	144
Number of training data pairs	355
Number of fuzzy rules	27

Table 7
Predicting performances of ANFIS model with different MFs for Zone-2.

Membership functions	RMS	R^2
Gbellmf-3	17.7293	0.9408
Gbellmf-2	17.7672	0.9405
Trimf-3	18.1279	0.9381
Trimf-2	19.9226	0.9252
Gaussmf-3	17.7024	0.9410
Gaussmf-2	17.7159	0.9409
Gauss2mf-3	**17.7019**	**0.9410**
Gauss2mf-2	19.8681	0.9256
Pimf-3	17.7965	0.9403
Pimf-2	42.8843	0.6535

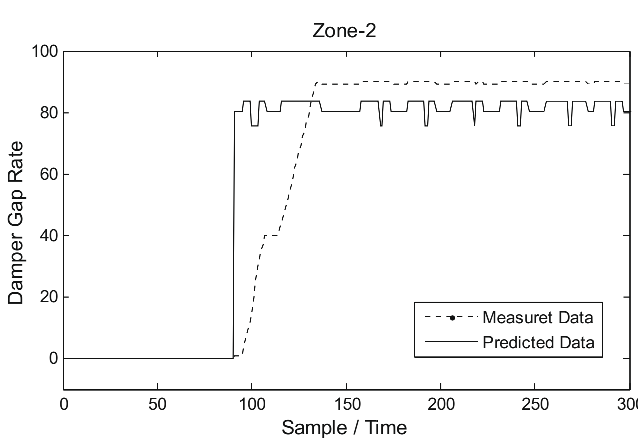

Fig. 13. Predicted and actual gap rate for Zone-2.

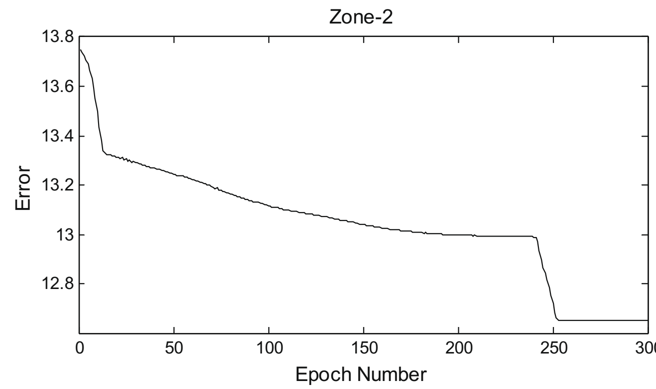

Fig. 14. Training performance of ANFIS model for Zone-1.

For modeling Zone-2; the formed ANFIS model was trained for 300 epochs and the structure of ANFIS model is presented in Table 6. The predicting performance is shown in Fig. 13. The realized simulations and their predicting performance by using different MF are tabulated in Table 7. Finally, the best performance was obtained with pi shaped MF. The RMS value is 17.7019 and the R^2 value is 0.9410. The training error is shown in Fig. 14.

6. Conclusions

In this study, the cooling process of the system was realized by being cooled the two different zones from the ambient temperature 26.4 °C to the desired temperatures. The required damper gap rates for obtaining the desired temperatures of two different zones and the required fan motor speed to minimize energy consumption for each time step were found by using PID control algorithm. As seen in Fig. 5–7, 9, 11 and 13, the experimental results have been presented in graphical form by using MATLAB Graphical Toolbox. In this work, the fan motor speed and the damper gap rates of a HVAC system with two zones were predicted by using ANFIS method. To assess the effectiveness of our proposal ANFIS, three computer simulation were developed on the MATLAB environment. The ANFIS results were given in the related tables. The simulation results have shown that the ANFIS can be used as an alternative prediction and control method for HVAC systems. In statistical analysis, the RMS value is 3.3475 and the R^2 value is 0.9954 for evaporator while the RMS value is 15.6750 and the R^2 value is 0.9402 for zone-1 and the RMS value is 17.7019 and the R^2 value is 0.9410 for zone-2 for the ANFIS model. This paper shows that the values predicted with the ANFIS can be used to predict fan motor speed and damper gap rate of HVAC system quite accurately. Therefore, faster and simpler solutions can be obtained based on ANFIS.

References

Aprea, C., Mastrullo, R., Renno, C., & Vanoli, GP. (2004). An evaluation of R22 substitutes performances regulating continuously the compressor refrigeration capacity. *Applied Thermal Engineering, 24*(1), 127–139.

Ayata, T., Çam, E., & Yıldız, O. (2007). Adaptive neuro-fuzzy inference systems (ANFIS) application to investigate potential use of natural ventilation in new building designs in Turkey. *Energy Conversion and Management, 48*(5), 1472–1479.

Bi, Q., Cai, W. J., Wang, Q. G., Hang, C. C., Lee, E. L., Sun, Y., et al. (2000). Advanced controller auto-tuning and its application in HVAC systems. *Control Engineering Practice, 8*, 633–644.

Huang, S., & Nelson, R. M. (1994). Rule development and adjustment strategies of a fuzzy logic controller for an HVAC system: Part 1-analysis. *ASHRAE Transaction, 100*(1), 841–850.

Hung, L. C., Lin, H. P., & Chung, H. Y. (2007). Design of self-tuning fuzzy sliding mode control for TORA system. *Expert Systems with Applications, 32*, 201–212.

Jang, J. S. R. (1993). ANFIS: Adaptive Network-Based Fuzzy Inference Systems. *IEEE Transactions on Systems Man and Cybernetics, 23*(3), 665–685.

Kalogirou, S., Eftekhari, M., & Marjanovic, L. (2003). Predicting the pressure coefficients in a naturally ventilated test room using artificial neural networks. *Building and Environment, 38*, 399–407.

Kaynakli, O., Pulat, E., & Kilic, M. (2005). Thermal comfort during heating and cooling periods in an automobile. *Heat and Mass Transfer, 41*(5).

Krakow, K. I., & Lin, S. (1995). PI control of fan speed to maintain constant discharge pressure. *ASHRAE Transactions: Research, 101*(Part 2), 398–407.

Kulakarni, A. D. (2001). *Computer vision and fuzzy neural systems*. NJ: Prentice Hall.

Lu, L., Wenjian, C., Lihua, X., Shujiang, L., & Chai, S. Y. (2005). HVAC system optimization-in-building section. *Energy and Buildings, 37*(1), 11–22.

Mamdani, EH. (1974). Application of fuzzylogic algorithms for control of simple dynamic plant. *Proceedings of the Institute of Electrical Engineering, 121*, 1585–1588.

McQuiston, F., & Parker, J. (1997). *Heating, ventilating, and air conditioning analysis and design*. New York: Wiley.

Pinnella, M. J., Wechselberger, E., Hittle, D. C., & Pederson, C. O. (1986). Self-tuning digital integral control. *ASHRAE Transactions, 86*(2), 202–210.

Riverol, C., & Pilipovik, M. V. (2005). Tuning a space–time scalable PI controller using thermal parameters. *Heat and Mass Transfer, 41*(5).

Seem, J. E. (1998). A new pattern recognition adaptive controller with application to HVAC systems. *Automatica, 34*(8), 969–982.

Shin, Y., Chang, Y. S., & Kim, Y. (2002). Controller design for a real-time air handling unit. *Control Engineering Practice, 10*, 511–518.

Tang, K. L., & Mulholland, R. J. (1987). Comparing fuzzylogic with classical controller designs. *IEEE Transactions on Systems Man and Cybernetics, 17*(6), 1085–1087.

Tassou, SA., & Quereshi, TQ. (1998). Comparative performance evaluation of positive-displacement compressors in variable-speed refrigeration applications. *International Journal of Refrigeration-revue Internationale du Froid, 21*(1), 29–41.

Teitel, M., Levi, A., Zhao, Y., Barak, M., Bar-lev, E., & Shmuel, D. (2008). Energy saving in agricultural buildings through fan motor control by variable frequency drives. *Energy and Buildings, 40*, 953–960.

Tsang, K. M. (2001). Auto-tuning of fuzzy logic controllers for self-regulating processes. *Fuzzy Sets and Systems, 120*, 169–179.

Yu, F. W., & Chan, K. T. (2006). Modelling of the coefficient of performance of an air-cooled screw chiller with variable speed condenser fans. *Building and Environment, 41*, 407–417.

Yu, F. W., & Chan, K. T. (2007). Modelling of a condenser-fan control for an air-cooled centrifugal chiller. *Applied Energy, 84*, 1117–1135.

Yu, F. W., & Chan, K. T. (2007). Part load performance of air-cooled centrifugal chillers with variable speed condenser fan control. *Building and Environment, 42*, 3816–3829.